ISSN: 0975-833X

Available online at http://www.journalcra.com

International Journal of Current Research
Vol. 9, Issue, 08, pp.55598-55605, August, 2017

INTERNATIONAL JOURNAL OF CURRENT RESEARCH

RESEARCH ARTICLE

REACTIVITY OF DEFECT-FREE AND VACANCY-CONTAINING HEXAGONAL GRAPHENE NANOCLUSTERS ACCORDING TO QUANTUM CHEMISTRY APPROACH

***,[1]Kartel, M.,[1]Karpenko, O., [1]Lobanov, V. and [2]Wang Bo**

[1]O. Chuiko Institute of Surface Chemistry, NASU, 17 General Naumov str., Kyiv03164, Ukraine
[2]China-Central and Eastern Europe International Science and Technology Achievement Transfer Center of Ningbo University of Technology, Ningbo 315211, China

ARTICLE INFO

Article History:
Received 25th May, 2017
Received in revised form
23rd June, 2017
Accepted 07th July, 2017
Published online 31st August, 2017

Key words:

Density functional theory,
Graphene nanoclusters,
Carbon nanoclusters.

ABSTRACT

By density functional theory method (B3LYP, basis 6-31G**) the equilibrium spatial structure and the electronic structure have been calculated of carbon nanoclusters (CNC) derived from the nanocluster C_{96} of hexagonal shape due to removing one or two atoms. For comparison, the calculations have been carried out of similar structures formed from polycyclic aromatic molecules (PAM) $C_{96}H_{24}$ due to removal on one or two carbon atoms also. It has been show that: the ground electronic states of CNC $C_{96\text{-}1(1)}$, $C_{96\text{-}2(1)}$, and $C_{96\text{-}1(1)}H_{24}$ systems are triplet, while that of the system $C_{96\text{-}2(1)}H_{24}$ - quintet; the creation of a monovacancy in the central hexagon of CNC C_{96} does not violate the isolation of the conjugated system of the peripheral chain of carbon atoms, as in the case of defect-free CNC C_{96} hexagonal structure; spectrum of single-electron energy levels of the clusters containing vacancies includes the energies of several frontier vacant MOs localized at the cyclic peripheral chain belonging into the range of energies of the highest occupied MO; the removal of one atom from the central hexagon CNC C_{96} results in a "friable" structure of the formed cluster $C_{96\text{-}1(1)}$, what is reflected in the reduction of the removal energy for the second carbon atom from the $C_{96\text{-}1(1)}$; removing carbon atom of PAM $C_{96}H_{24}$ stabilizes the resulting system what is evidenced by the growth of the formation energy of the second monovacancy compared to that of the first one; the properties of CNC containing vacancies differ from those of the systems obtained from PAM due to removal of carbon atoms.

Citation: Kartel, M., Karpenko, O., Lobanov, V. and Wang Bo, 2017. "Reactivity of defect-free and vacancy-containing hexagonal graphene nanoclusters according to quantum chemistry approach", *International Journal of Current Research*, 9, (08), 55598-55605.

INTRODUCTION

Prior to the development of methods for obtaining two-dimensional single-layer lattice of carbon atoms in a sp^2-hybridized state (graphene) (Novoselov *et al.*, 2004), quite reasonable assumptions were made about the possibility of replacing silicon with carbon in the element base of microelectronics and the prospects for transition to molecular electronics (Van Noorden *et al.*, 2006). The prerequisites for this were extremely high rate of electron transfer, display of the Hall effect at room temperature and several other electronic properties of graphene (Aberger *et al.*, 2010). These properties were found by theoretical calculations (Wallace *et al.*, 1956) within the tight binding approximation (Slater *et al.*, 1954), which is used in solid state theory (Cox *et al.*, 1987). However, graphene itself, as an infinite two-dimensional system of carbon atoms in sites of regular hexagons, is of little use in the electronics, due to the zero density of states at the Fermi level and the lack of band gap.

Corresponding author:* **Kartel, M.
O. Chuiko Institute of Surface Chemistry, NASU, 17 General Naumov str., Kyiv03164, Ukraine.

In principle, it is possible to avoid the shortcomings in several ways, including: the transition to a finite graphene-like system, i.e. the introduction of a certain type of frontiers; creating sets of one- or polyatomic vacancies; inclusion of heteroatoms into the lattice of carbon atoms; violation of the periodic structure. A combination of several or all of methods is also taken into account.Thus, it has been shown in some experimental (Ponomarenko *et al.*, 2008; Katsnelson *et al.*, 2006) and theoretical (Viana-Gomes *et al.*, 2009; Ma *et al.*, 2004) works that nanometer-sized carbon clusters with graphite-like structure have several unique properties that are not inherent in the bulk samples of different carbon allotropes. First of all, it refers to the manifestation of magnetism in polymerized fullerene (Makarova *et al.*, 2001) and irradiated graphite (Esquinazi*et al.*, 2002), what stimulated the study of physical and chemical properties of various nanosystems containing only carbon atoms, in order to create light non-metallic magnets with the Curie point in the range of room temperature. In the above mentioned and some other theoretical studies (Pykal *et al.*, 2016; Kazubov *et al.*, 2012; Sheka *et al.*, 2012), computational quantum chemistry methods have been involved. The results of their application have elucidated that a

decisive role, together with the form and type of boundaries that limit carbon cluster, is played at by different kinds of defects in the crystal structure, especially monoatomic vacancies. An interest to the study of the properties of graphite containing vacancies arose in connection with its use in nuclear reactors as a neutron moderator, long before the development of the methods for reproduction graphene samples. As a model, single-layer carbon nanoclusters (CNC) with graphite-like structure were considered. Especially the rapid development of these works begun after the realization of an idea that the hexagon monatomic layer of carbon atoms can be considered as a single structural element of many hybridized sp^2-carbon structures. The results obtained both experimentally and by various modeling techniques, including quantum chemical ones, revealed the impact of the presence of defects (vacancies) of different types on the electronic (Viana-Gomes *et al.*, 2009), thermal (Chernozatonskii *et al.*, 2007), and mechanical (Coronado *et al.*, 2001) properties of graphite-like clusters and on their reactivity and catalytic activity (Ma *et al.*, 2004).

When using quantum-chemical methods, a choice is critical of models that reproduce the system in question. Thus, when calculating the CNC, in some cases carbon atoms located at the periphery of the cluster, are saturated with hydrogen atoms to compensate for edge effects, but is taken to consider actually some polyaromatic molecule. Therefore, along with the main goal - finding the properties of CNC containing carbon vacancies – indirectly, but equally important is to compare their properties with those of polycyclic aromatic molecules (PAM) of similar structure.In our previous paper (Karpenko *et al.*, 2013) devoted to the study of quantum chemical properties of the ideal (containing no defects) CNC of hexagonal structure, it has been shown that limited cluster structure C_{96} can adequately convey the properties of carbon nanoclusters of finite size with zigzag boundaries. Also it has been found that the electronicground state (EGS) of ideal CNC C_{54}–C_{216} of hexagonal shape, despite an even number of electrons in them, is not singlet, namely triplet or quintet, and is determined by even or odd number of double coordinate carbon atoms ($C^{(2)}$) in each identical boundary respectively. Also, the calculations have shown that the spectrum of single-electron energy levels is such that some of them corresponding to the lowest unoccupied molecular orbitals (LUMO) fall into the range of energies of the highest occupied molecular orbital (HOMO).

This applies to the frontier LUMO focused on both the chemical bonds around entire cluster and on the limiting chain atoms. Placing electrons on them does not ensure the implementation of localized states in the peripheral, i.e. located at the border, twice coordinated carbon atoms.In the paper there been calculated by density functional theory method (DFT) (Kohn *et al.,* 1965; Parr *et al.*, 1989) (exchange-correlation functional B3LYP, basis set 6-31 G **) the equilibrium configurations and corresponding total energy values of carbon clusters that can be considered as quantum nanodots obtained by removing one ($C_{96\text{-}1(1)}$) or two non-adjacent ($C_{96\text{-}2(1)}$) carbon atoms from the CNC C_{96} of ideal hexagonal shape. For comparison similar structures have been considered formed by removal of one ($C_{96\text{-}1(1)}H_{24}$) or two ($C_{96\text{-}2(1)}H_{24}$) carbon atoms from PAM $C_{96}H_{24}$. The most of the available literature data on the structure and properties of this type (Viana-Gomes *et al.*, 2009; Ma *et al.*, 2004) were obtained by just this method.

RESULTS AND DISCUSSION

All the systems are tested under conditions of multiplicity M=1, 3, 5, and in some cases in the state with M=7. The calculation results are shown in Table 1, which shows that the EGS of CNC containing different types of vacancies, is not singlet, that is, for them as well as for defect-free CNC C_{96} spin polarization is observed. For reference energy level for each of the systems the EGS energy has been selected.The bond lengths of the equilibrium configuration of CNC $C_{96\text{-}1(1)}$ in EGS (M=3) are shown in Fig. 1, which illustrates that the removal of one carbon atom from the central hexagon of defect-free CNC C_{96} has no effect practically on the structure of the peripheral cyclic chain.

Table 1. Energies (eV) of the systems considered for the different spin states*

Multiplicity (M)	System				
	C_{96}	$C_{96\text{-}1(1)}$	$C_{96\text{-}2(1)}$	$C_{96\text{-}1(1)}H_{24}$	$C_{96\text{-}2(1)}H_{24}$
1	7.66	8.01	8.95	0.87	1.73
3	1.65	0	0	0	0,68
5	0	0.63	0.93	1.37	0
7	1.05	--	--	--	1.47

*Dashes in a row referring to septet states mean that the systems in this state are not considered, since it has been revealed that their ground electronic states are triplet.

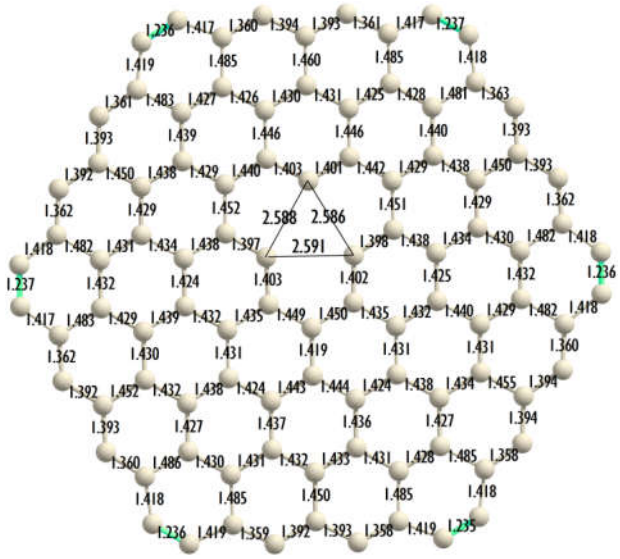

Figure 1. The C−C bond lengths and the distances between the carbon atoms surrounding the vacancy in the CNC $C_{96\text{-}1(1)}$ (M=3)

As in case for C_{96} (M=5) (Karpenko *et al.*, 2013), in the contact zigzag of edges peripheral cyclical chain, the carbon-carbon bond lengths are of 1.235−1.237 Å, what is slightly different from the bond length in acetylene (1.212 Å), and in each seven-atomic edge fragments, there are significantly altering bond lengths. The bond lengths between the atoms of peripheral cycle chain and the nearest atoms of the internal part of cluster are in the range of 1.450 to 1.485 Å. This leads to the isolation of the conjugated system of peripheral chain from the similar system of central part of CNC, allowing us to believe them to be relatively independent. The essential feature of the spatial structure at CNC $C_{96\text{-}1(1)}$ in the triplet state is an increase in the distances between the carbon atoms surrounding the vacancy to 2.588−2.591 Å compared to CNC C_{96} where they are of 2.478−2.486 Å. This result is contrary to the data cited in some studies.

For example, in (El-Barbary*et al.*, 2003) within the DFT approximation for PAM $C_{120}H_{27}$ in the singlet state it was found that after the formation of vacancies, a convergence took peace of two adjacent carbon atoms to the distance of 2.1 Å, so forming a pentagon. However, as it can be seen from the Table 1, the singlet state of the CNC $C_{96\text{-}1(1)}$ is for 8.01 eV above the triplet one. A similar result (DFT approximation, imposing periodic conditions) was obtained in (Ma *et al.*, 2004), where in the area of vacancy a pentagon is created, one of the bond lengths being of 2.2 Å. This work also anticipates that the EGS of CNC is singlet. Increased C···C distances in the CNC $C_{96\text{-}1(1)}$ (M=3) around vacancies apparently can be explained by taking into account of the distribution of spin density (σ). Fig. 2 shows that on all the doubly coordinated carbon atoms surrounding the vacancy the spin densities are of the same sign. In addition, the atomic charges are positive and have, as for the system consisting only of atoms of the same type, rather high amount equal to 0.2 a.u.

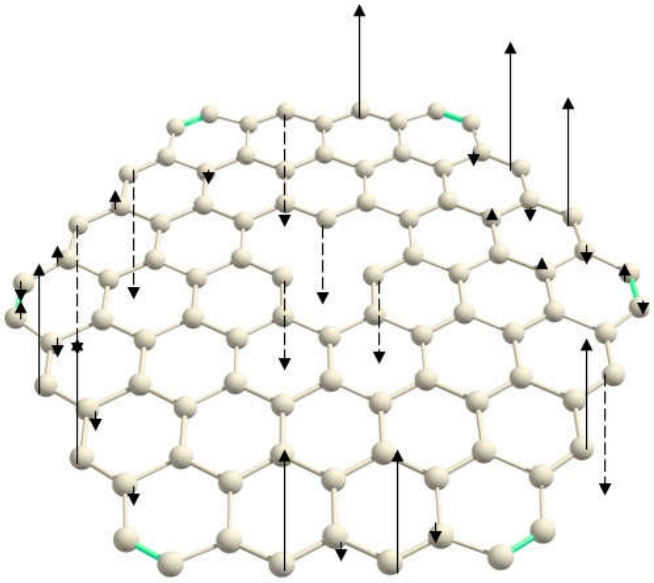

Figure 2. The spin density distribution in CNC $C_{96\text{-}1(1)}$ (M=3). The solid arrows show the σ distribution of α-subsystem, dotted ones – that of β-subsystem. The arrow lengths are proportional to the spin density

A somewhat different situation occurs in the formation of similar vacancy in the PAM $C_{96}H_{24}$. First of all, note that for the system $C_{96\text{-}1(1)}H_{24}$, the ground electronic states is also triplet (M=3), but the energy gap between the triplet and singlet state is almost ten times smaller than that in the case of CNC C_{96} (see Table 1). At the equilibrium configuration of the system $C_{96\text{-}1(1)}H_{24}$ (M=3) (see Fig. 3), between two carbon atoms surrounding the vacancy, a weak covalent bond occurs with length of 1.909 Å, what leads to the formation of a pentagon. In this system, the C−C bonds lengths at the turn of zigzag edges are up 1.358−1.364 Å, which allows one to believe them to be double bonds. The bond lengths between the peripheral carbon atoms and atoms inside of the system are much shorter than those in the cluster $C_{96\text{-}1(1)}$ and are in the range of 1.431−1.443 Å.

This suggests that removing one atom from the central hexagon of $C_{96\text{-}1(1)}H_{24}$ molecule does not lead to the separation of π-conjugated system of regional chain of atoms from the similarly π-conjugated system of the central part.

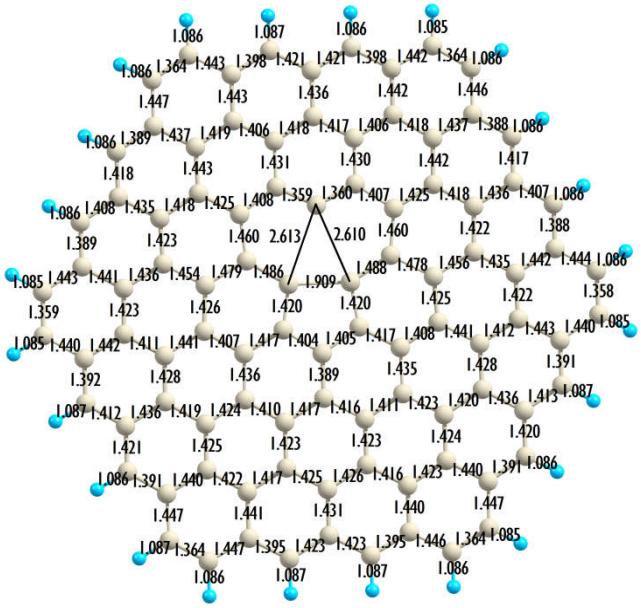

Figure 3. The C−C and C−H bond lengths in the equilibrium configuration of the system$C_{96\text{-}1(1)}H_{24}$ (M=3)

Otherwise, compared to CNC $C_{96\text{-}1(1)}$, the spin density is distributed around the vacancy created in PAM $C_{96}H_{24}$, i.e. the system $C_{96\text{-}1(1)}H_{24}$. Thus, at one of three atoms surrounding the vacancy, namely at that which is not involved in the formation of a pentagon, the value of spin density is 1.2 a.u., while the nearest atoms have alternating signs (Fig. 4), and the absolute value is within 0.1 a.u.

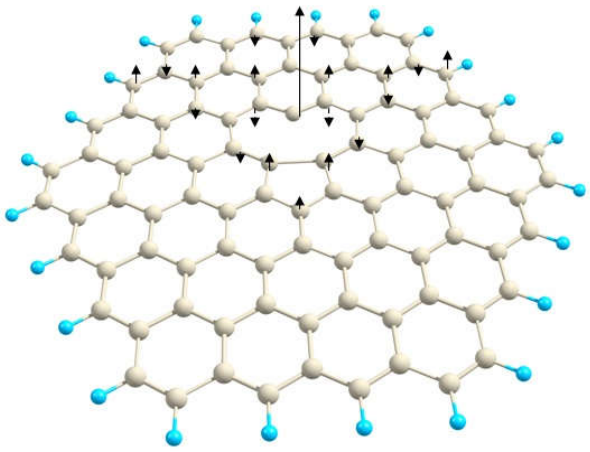

Figure 4. The σ distribution in the system$C_{96\text{-}1(1)}H_{24}$ (M=3). The arrows directed upwards show the σ distribution in α-subsystem; downward − that in β-subsystem. The lengths of the arrows are proportional to the spin density

Obviously, such a difference compared with the distribution in CNC $C_{96\text{-}1(1)}$ is due to the lack of twice coordinated atoms at the periphery of the system $C_{96\text{-}1(1)}H_{24}$, where the spin density is mainly focused.For CNC $C_{96\text{-}1(1)}$, as for defect-free cluster C_{96}, the order of filling the one-electron energy levels (ε_i) with electrons is affected by the presence of doubly coordinated atoms in the system on the periphery of the cluster and around the vacancy. It appears in fact that in part of the spectrum referred to the frontier molecular orbitals (MOs), some MOs, with energy below the HOMO one are empty (see Fig. 5).

This refers to the MOs, distributed through chemical bonding cycle of peripheral chain. One of such MOs of α-subsystem (α287) is shown in Fig. 6; its energy is lower that the energies of occupied MOs (α279-α286) having the same type of structure. The same type of structure is reflected in their preferred location at one of the atoms $C^{(2)}$ of peripheral chain (Fig. 6). Similar findings are true also for the MOs of β-subsystem.

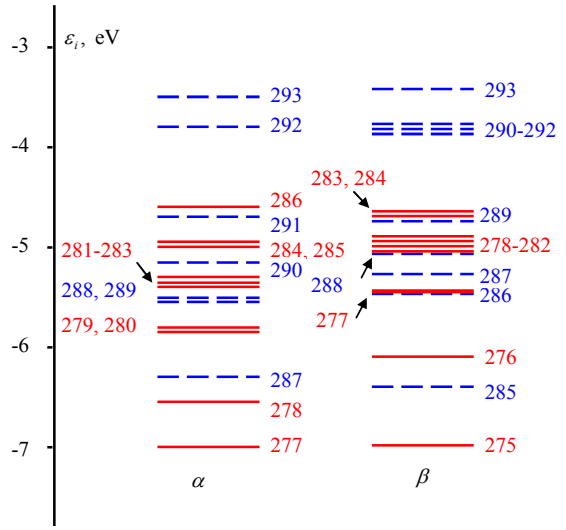

Figure 5. Scheme of single-electron energy levels of α-and β-subsystems of GES of the CNC$C_{96\text{-}1(1)}$ (solid lines depict the energy levels of occupied MO, dashed ones − vacant)

The impact of the presence of incompletely coordinated atoms in the system, and therefore, of their localized electronic states on the order of filling single-electron energy levels is clearly evident, when comparing the ε_i spectra of CNC $C_{96\text{-}1(1)}$ and those of the clusters obtained by removing one electron from it (cluster $[C_{96\text{-}1(1)}]^+$), or addition of one electron (cluster $[C_{96\text{-}1(1)}]^-$). Comparing Figs. 5 and 7, it can be concluded that as a result of ionization of the CNC $C_{96\text{-}1(1)}$, electron leaves HOMO α286, which in the original cluster was localized at one of the $C^{(2)}$ atoms (Fig. 6). In the GES of ionized cluster $[C_{96\text{-}1(1)}]^+$ (M=2) the structure of this orbitals is different and it appears to be distributed over peripheral chemical bonds (Fig. 8). This delocalization is not consistent with the presence of type $C^{(2)}$ atoms in the system $[C_{96\text{-}1(1)}]^+$ which are characterized by their localization in one-electron states. Therefore, despite its not occupancy, the corresponding energy level gets the energy range of higher occupied MOs (see Fig. 7).

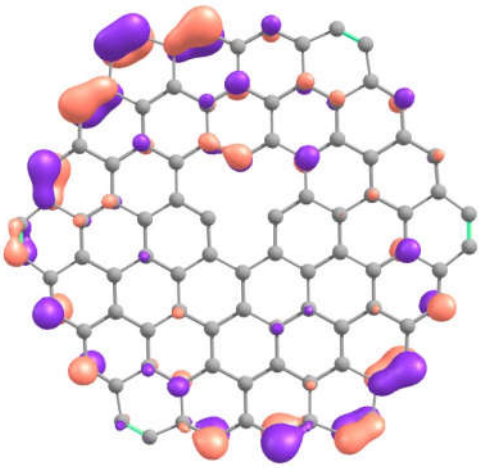

α **287**

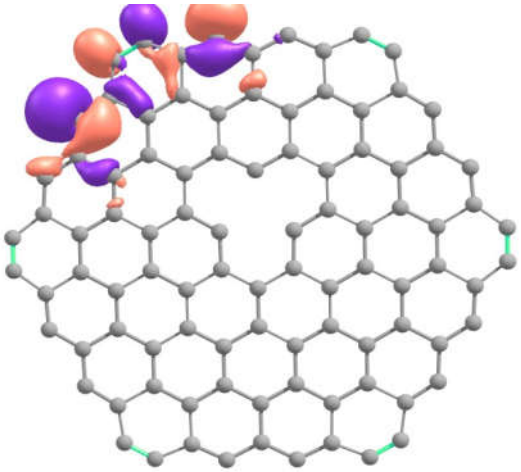

α **286**

Figure 6. The structure of the lowest unoccupied (*α*287) and the highest occupied (*α*286) MOs of CNC $C_{96\text{-}1(1)}$

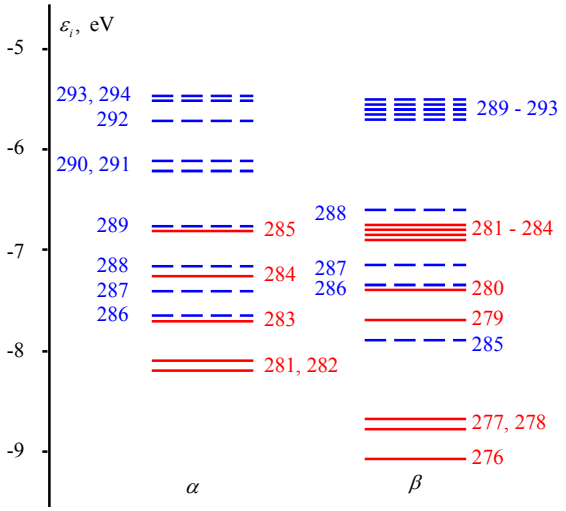

Figure 7. Scheme of single-electron energy levels of α-and β-subsystems of GES of CNC $[C_{96\text{-}1(1)}]^+$ (solid lines depict the energy levels of occupied MO, dashed − vacant)

Another picture is observed when joining electron to the cluster $C_{96\text{-}1(1)}$, where the lowest energy level is vacant β285 MO (Fig. 7) distributed over eight chemical bonds (see Fig. 8). Placement of electron on this orbital leads to the fact that in the anion $[C_{96\text{-}1(1)}]^-$ it is already occupied (Fig. 9) and localized, and its structure (Fig. 8) is consistent with the presence of atoms on the periphery of the system with the electronic states focused on them.

When removing two carbon atoms from the first cycle chain of CNC C_{96}, a cluster is formed (Fig. 10 *a*), its GES being triplet (see Table 1) and its equilibrium structure unlike that of the cluster $C_{96\text{-}1(1)}$ with monovacancy is characterized by the presence of two pentagons. Bond lengths between pairs of atoms that form each of the pentagon are of 1.964 Å. They can be attributed to rather weak ones, due to the positive charges (0.24 a.u.) on these atoms. Spin densities in each of the three carbon atoms, as well as in the case of a monovacancy, have the same sign and are preferentially localized on the doubly coordinated atoms around vacancies (Fig. 11 *a*).

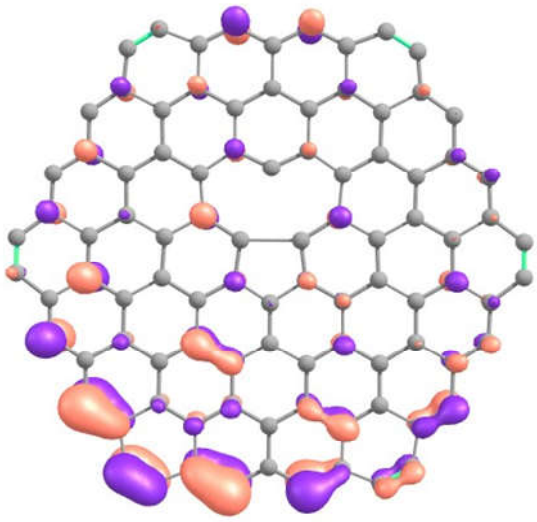

α **286** in $[C_{96\text{-}1(1)}]^+$

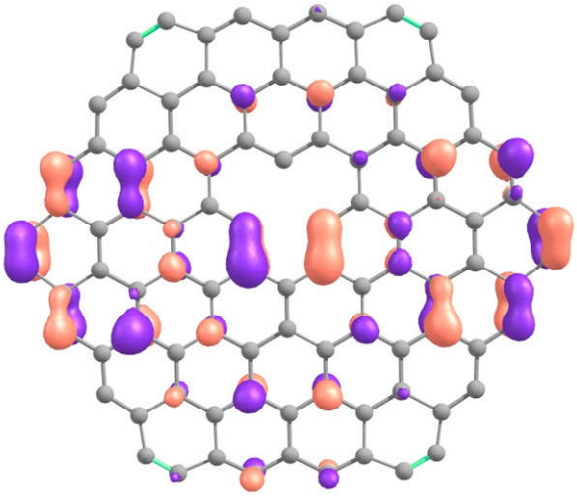

β **285** in $C_{96\text{-}1(1)}$

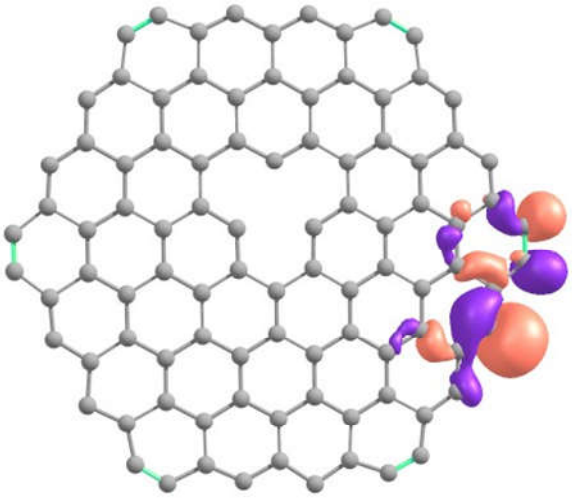

β **285** in $[C_{96\text{-}1(1)}]^-$

Figure 8. The MOs structures: α286 in $[C_{96\text{-}1(1)}]^+$;β285 in $C_{96\text{-}1(1)}$;β285 in $[C_{96\text{-}1(1)}]^-$

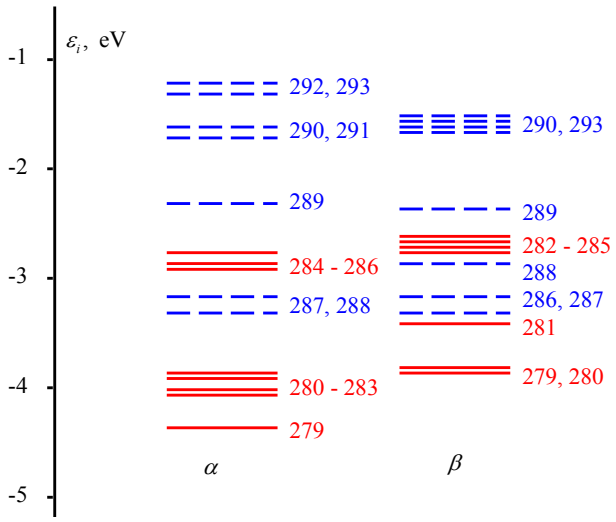

Figure 9. The scheme of single-electron energy levels of α-and β-subsystems of GES of CNC $[C96\text{-}1(1)]^-$ (solid lines depict the energy levels of occupied MOs, dashed – those of vacant ones)

For a similar structure system $C_{96\text{-}2(1)}H_{24}$ formed by the removal of its two carbon atoms from it the GES is quintet (M=5) (see Table 1). In this case, it is also characterized by the formation of two pentagons, but the distance between adjacent carbon atoms is for almost 0.2 Å smaller than that in the cluster $C_{96\text{-}2(1)}$ (M=3). The distribution of spin density over the atoms (Fig. 11 *b*) surrounding each of vacancies in the system $C_{96\text{-}2(1)}H_{24}$ (M=5) generally coincides with the analogous distribution around monovacancy in the system $C_{96\text{-}1(1)}H_{24}$ (M=3).

Table 2 shows total energy values of the systems considered in their ground electronic state, so one can get information on estimated removal energy of carbon atoms from the CNC C_{96} and PAM $C_{96}H_{24}$. (When calculating the total energy of an isolated carbon atom in the triplet state was believed to be equal to 37.843662 a.u.).

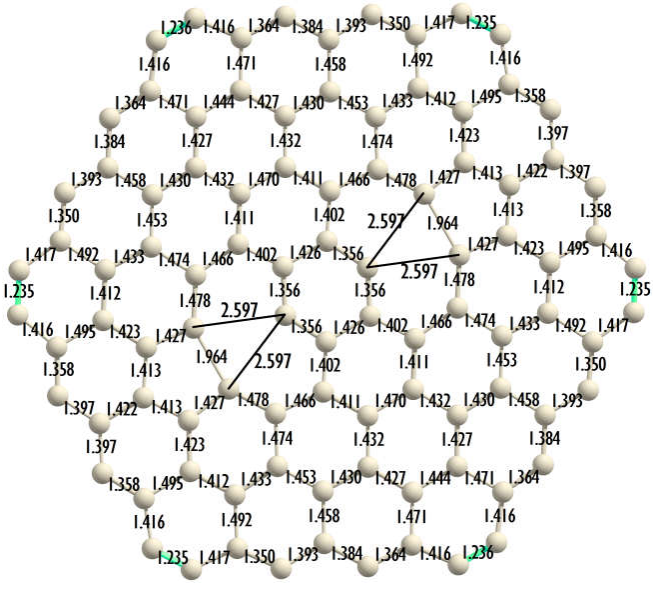

a

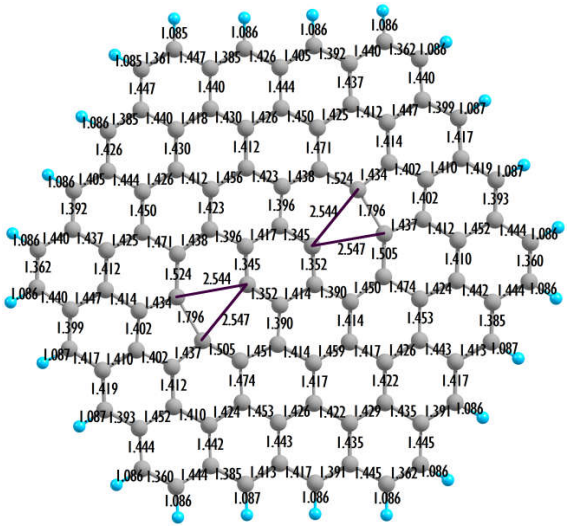

b

Figure 10. Equilibrium spatial structure of CNC $C_{96\text{-}2(1)}$ (M=3) (*a*) and of system $C_{96\text{-}2(1)}H_{24}$ (M=5) obtained from PAM $C_{96}H_{24}$ due to removal of two carbon atoms (*b*)

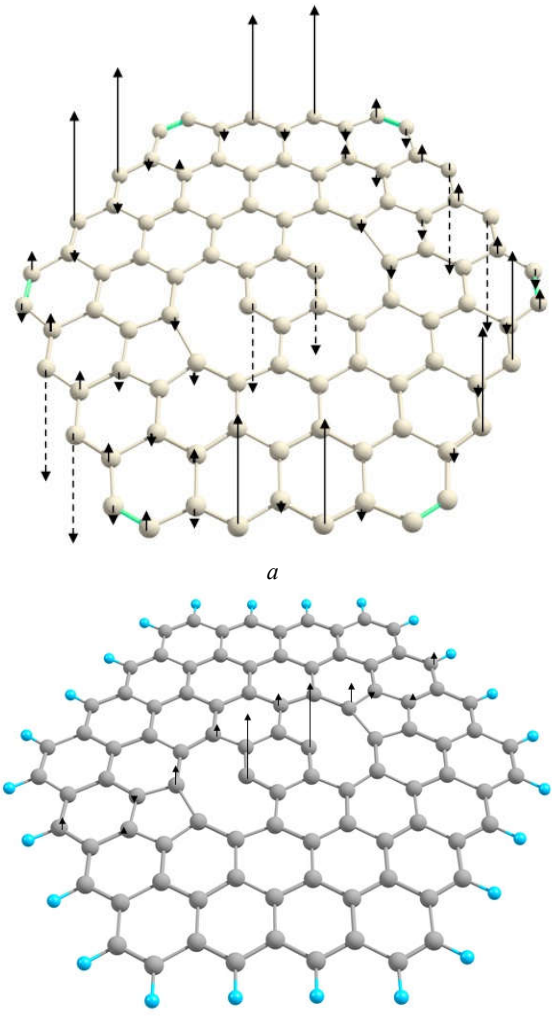

a

b

Figure 11. The spin density distribution in the CNC $C_{96\text{-}2(1)}$ (M=3) (*a*) and in the system$C_{96\text{-}2(1)}H_{24}$ (M=5) (*b*) obtained from PAM $C_{96}H_{24}$ due to removal of two carbon atoms

The removal of single atom from CNC C_{96} needs an energy consumption of 1572.4 kJ/mol (16.3 eV), equivalent to that calculated for three bonds simultaneously broken (524.1 kJ/mol). The formation of CNC $C_{96\text{-}2(1)}$ (M=3) one from the cluster $C_{96\text{-}1(1)}$ (M=3) is accompanied by the energy effect of 1342.6 kJ/mol (13.9 eV) that in terms of one broken bond gives the value of 320.9 kJ/mol. This reduction in energy consumed to remove the second carbon atom indicates a destabilization of the cluster $C_{96\text{-}1(1)}$ compared to initial CNC C_{96}, so that, the second one can be considered crumblier. An additional argument in favor of the assumption may be increasing the distance (*D*) between the two most distant from each other carbon atoms to 17.34 Å in the CNC with monovacancy compared to 17.14 Å in the CNC C_{96}.

Table 2. The total energy values (a.u.) of CNC C_{96}, PAM $C_{96}H_{24}$ and the related systems produced by removing one or two carbon atoms

	Energy systems		
	No vacancy	One vacancy	Two vacancies
CNC C_{96}	- 3656.225213	- 3617.781952	- 3579.426596
PAM $C_{96}H_{24}$	- 3672.550987	- 3634.149517	- 3595.680933

When removing a carbon atom from PAM $C_{96}H_{24}$, breaking one C−C bond consumes the energy of 447.8 kJ/mol, the formation of the second monovacancy increases this value to 490.5 kJ/mol. The increase in the average energy of C−C bond in the system $C_{96\text{-}1(1)}$ (M=3) compared to that for the original PAM $C_{96}H_{24}$ correlates with a decrease in the *D* value when transiting from $C_{96}H_{24}$ to $C_{96\text{-}1(1)}H_{24}$. In this regard it is important to note that the above mentioned numerical values of the formation energy monovacancy in CNC and PAM should not be considered absolute, since they depend on the locations where carbon atoms are removed and mutual effect of the vacancies. The presences of the localized triple ($CNCC_{96}$) and double ($PAMC_{96}H_{24}$) carbon-carbon bonds testifies apossibility of their participation in the reactions of electrophilic addition. Incase of PAM, the reactions of substitution are also eventual. When attacking an unsaturated bond, a reagent molecule is considerably polarizedin the vicinity. Thedegree of such polarization can be found from the molecular electrostatic potential (ρ) distributions shown in the Fig. 12. It is seen from the Fig. 12*a* that in plane of CNC C_{96} (X0Y plane), neareach of the triple bonds a compactarea of negative values of potential is localized. It follows from the distribution of electrostatic potential within the Z0Y plane (perpendicular to the X0Y plane and passing through the centers of a pair of peripheral triple bonds (Fig.12*b*), that the area of negative ρ values is spread to in finitely large distance from the centers of negative charge. It concedes a possibilityof a barrier-free access of cations andsmall proton donor moleculestotriple bonds. Availability of a single vacancy in the cluster $C_{96\text{-}1(1)}$ leads to expansion of the negative electrostatic potential values (see Fig. 13) and to an increase in the absolute values in the sites of localization of its minimum. This indicates an increase in proton acceptor properties of the $C_{96\text{-}1(1)}$ compared to those of the defect-free CNC C_{96}.

Thus, despite the CNC C_{96} and $C_{96\text{-}1(1)}$ consists of only one type atoms (carbon atoms), the distribution of molecular electrostatic potential in their vicinity is far from homogeneity. Such anisotropy in ρ distribution causes a specific behavior of CNC towards proton donor reagents as well as electron donor ones. Besides, the idea about distribution of molecular electrostatic potential allows us getting an evident and unambiguous specification of the centers of primary interaction between CNC and polar molecules.

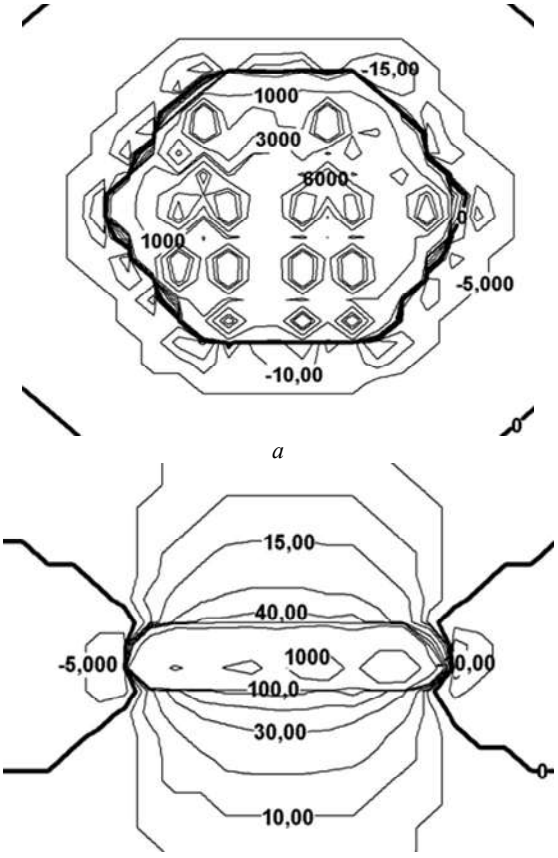

Figure 12. Distribution of ρ (kJ/mol) in the plane of the CNC C_{96} (*a*),and in a plane perpendicular to the CNC (*b*)

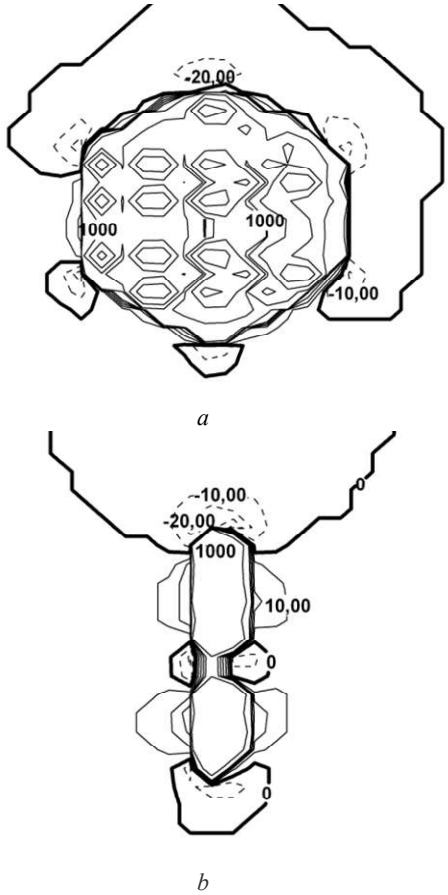

Figure 13. Distribution of ρ (kJ/mol) in the plane of the CNC $C_{96\text{-}1(1)}$ (*a*),and in a plane perpendicular to the CNC (*b*)

Conclusion

1. It follows from the results of the calculations that GES of carbon nanoclusters, obtained from CNC C_{96} with ideal hexagonal shape or from PAM $C_{96}H_{24}$ due to formation of one or two monovacancy despite an even number of electrons in these systems, is not singlet.
2. The spatial structure of CNC $C_{96\text{-}1(1)}$ and $C_{96\text{-}2(1)}$ is such that the orbital $2p_z$ of cyclic the edge chains form a conjugated system, poorly bonded with the π-system of the central part of cluster. This suggests that the chain is relatively isolated, and does not participate in the formation of a united conjugated system of the cluster. For $C_{96\text{-}1(1)}H_{24}$ and $C_{96\text{-}2(1)}H_{24}$ derived from PAM $C_{96}H_{24}$, the introduction of one or two mono vacancies does not violate the united conjugated system.
3. For the spectrum of single-electron energy levels of CNC $C_{96\text{-}1(1)}$ and $C_{96\text{-}2(1)}$, as for the CNC C_{96} it is characteristic that some MO distributed over bonds of the edge cyclic chain remain vacant, although relative energy levels are lower than those of some occupied MOs.
4. The formation energies of one and two vacancies in the CNC C_{96} and $C_{96}H_{24}$ show "loosening" structure due to transition from C_{96} to $C_{96\text{-}1(1)}$, while the introduction of a vacancy in the PAM $C_{96}H_{24}$ "plumps" the structure.
5. Modeling CNC with peripheral doubly coordinated carbon atoms by polycyclic aromatic molecules with hydrogen atoms, which saturate dangling bonds of peripheral carbon atoms, cannot properly mimic their structure and properties, what is true for nanoclusters with perfect hexagonal shapes, and for the clusters are containing vacancies.

REFERENCES

Aberger D., Apalkov V., Berashevich J., Zieler K., Chakraborty T. 2010. Properties of graphene: a theoretical perspective. *Adv. Phys*., 59(4):261–482.

Chernozatonskii L.A., Sorokin P.B., Brüning J.W. 2007. Two-dimensional semi conducting nano structures based on single grapheme sheets with lines of adsorbed hydrogen atoms. *Appl.Phys.Lett*., 91:183103–183105.

Coronado E., Galán-Mascarós J.R., Gómez-García C.J., Laukhin V. 2001. Coexistence of ferromagnetism and metallic conductivity in a molecule-based layered compound. *Nature*, 408(681):447–449.

Cox P.A. 1987. The electronic structure and chemistry of solids. *Oxford, OxfordUniversity Press*, 259.

El-Barbary A.A., Telling R.H., Ewels C.P., Heggie M.I., Briddon P.R. 2003. Structure and energetics of the vacancy in graphite. *Phys. Rev. B*., 68(14):144107–144113.

Esquinazi P., Setzer A., Höhne R., Semmelhack C., Spemann D., Butz T., Kohlstrunk B., Lösche M. 2002. Ferromagnetism in oriented graphite samples. *Phys. Rev. B*., 66(2):024429–024438.

Jiang D., Sumpter B.G., Dai S. 2007. The unique chemical reactivity of agraphe nenanoribbon's zigzagedge. *J. Chem.Phys*., 126:134701–134711.

Karpenko O.S., Lobanov V.V., Kartel N.T. 2013. Properties of hexagon-shaped carbon nanoclusters. *Chem.Phys. Technol. Surf*., 4(2):123–131.

(DOI: https://doi.org/10. 15407/hftp04.02.123)

Katsnelson M.I., Novoselov K.S., Geim A.K. Chiral tunneling and the Klein paradox in graphene. 2006. *Nature Physics*, 2:620–625.

Kazubov A.A., Anan'eva Yu.A., Fedorov A.S., Tomilin F.N., Krasnov P.O. 2012. Quantum-chemical calculations on the stability and mobility of vacancies in grapheme. *Rus. J. Phys. Chem*., 86(7):1088–1099.

Kohn W., Sham L.S. 1965. Self-consistente quation including exchangeandcorrelationeffect. *Phys.Rev.A*., 140(4):1133–1138.

Ma Y., Lehtinen P.O., Foster A.S., Nieminen R.M. 2004. Magnetic properties of vacancies in graphene and single-walled carbon nanotubes. *New J. Phys*., 6(68):1–15.

Makarova T.L., Sundqvist B, Höhne R., Esquinazi P., Kopelevich Y., Scharff P., Davydov V.A., Kashevarov L.S., Rakhmanina A.V. 2001. Magnetic carbon. *Nature*, 413:716–718.

Novoselov K.S., Geim A.K., Morozov S., Jiang D., Zhang Y., Duboros S., Grigorieva I., Firsov A. 2004. Electric field effect in atomically thin carbon films. *Science*, 306(5696): 666–669.

Parr R.G., Yang W. Density-function altheoryofatoms andmolecules.1989.*Oxford:OxfordUniv. Press,* 333.

Ponomarenko L.A., Schedin F., Katsnelson M.I., Yang R., Hill E.W., Novoselov K.S., Geim A.K. 2008. Chaotic Dirac billiard in graphene quantum dots. *Science*, 320(5874): 356–358.

Pykal M., Jurecka P., Karlicky F., Otyepka M. Modeling of graphene functionalization. 2016. *Phys. Chem.Chem.Phys.*, 18:6351–6372.

Sheka E.F. 2012. Computation strategy for grapheme: Insight from odd electron correlation. *Inter. J. Quantum. Chem*., 112(18):3076–3090.

Slater J.C., Koster G.F. 1954. Simplified LCAO method for the periodic potential problem. *Phys. Rev*., 94(11):1498–15244.

Van Noorden R. Moving towards a grapheme world. 2006. *Nature*, 442(7170):228–229.

Viana-Gomes J., Pereira V.M., Peres N.M.R. 2009. Magnetism in strained graphene dots. Phys. Rev. B, 80(24):245436–245446.

Wallace P.R. The band theory of graphite. 1956. *Phys. Rev.*, 104(9):622–634.

****